

HYDROGEN EXPLOSIONS IN 20' ISO CONTAINER

Sommersel, O.K.¹, Vaagsather, K.² and Bjerketvedt, D.³

¹Telemark University College, Kjolnes Ring 56, Porsgrunn, N-3918, Norway, oksommersel@gmail.com

²Telemark University College, Kjolnes Ring 56, Porsgrunn, N-3918, Norway, knut.vagsather@hit.no

³Telemark University College, Kjolnes Ring 56, Porsgrunn, N-3918, Norway, dag.bjerkevedt@hit.no

ABSTRACT

This paper describes a series of explosion experiments in inhomogeneous hydrogen air clouds in a standard 20' ISO container. Test parameter variations included nozzle configuration, jet direction, reservoir back pressure, time of ignition after release and degree of obstacles. The paper presents the experimental setup, resulting pressure records and high speed videos. The explosion pressures from the experiments without obstacles were in the range of 0.4 to 7 kPa. In the experiments with obstacles the gas exploded more violently producing pressures in order of 100 kPa.

1.0 INTRODUCTION

With increasing interest in hydrogen safety the recent years, a strong effort has been made to learn more about hydrogen dispersion and explosions. Some examples of this work are reported by Shirvill et.al [1], Alcock et.al [2] and Takeno et.al. [3]. Computational Fluid Dynamics (CFD) codes calculating dispersion and flame propagation are necessary tools for performing safety studies. Validation and benchmarking of these codes have been reported in Papanikolaou et.al. [4], Giannissi et.al. [5] and Middha and Hansen [6], among many others.

This article describes the experiments that were performed at the NDEA test facility at Raufoss, Norway, June 2005, as part of an IEA-HIA task 19 project on hydrogen safety. The test series consisted of calibration experiments with C-4 high explosives and 39 gas explosions experiments with inhomogeneous hydrogen air clouds in an ISO container. The results consisted of pressure records and high-speed videos. The first 37 experiments were performed with an empty container, and with both the doors open. In experiments 38 and 39 the container were filled with obstacles, respectively 2 and 8 ordinary euro pallets. The explosion pressures from the experiments without obstacles were relatively low, in the range of 0.4 to 7 kPa. In the two experiments with obstacles the gas exploded more violently. The objective of this paper is to present a set of experimental data of a meso-scale experimental campaign with inhomogeneous hydrogen-air clouds.

2.0 EXPERIMENTAL SETUP

2.1 Module geometries

The hydrogen experiments were performed in a standard 20" ISO container, shown in Figure 1. The container had inner dimensions $L = 6$ m, $W = 2.4$ m and $H = 2.4$ m, and the steel walls and roof were corrugated. The doors shown on the container left hand side could be fully opened, whereas the end wall was solid (right side).



Figure 1. Image of the container used in the experiments

The container was placed approximately 30 meters from a shooting range bunker, where the instruments and high speed video cameras were set up. Figure 2 and Figure 3 show a schematic overview of the container with lengths and pressure monitor placements. Two large web bands were used to tie the container to the ground. The gas filling system was placed behind the closed end wall.

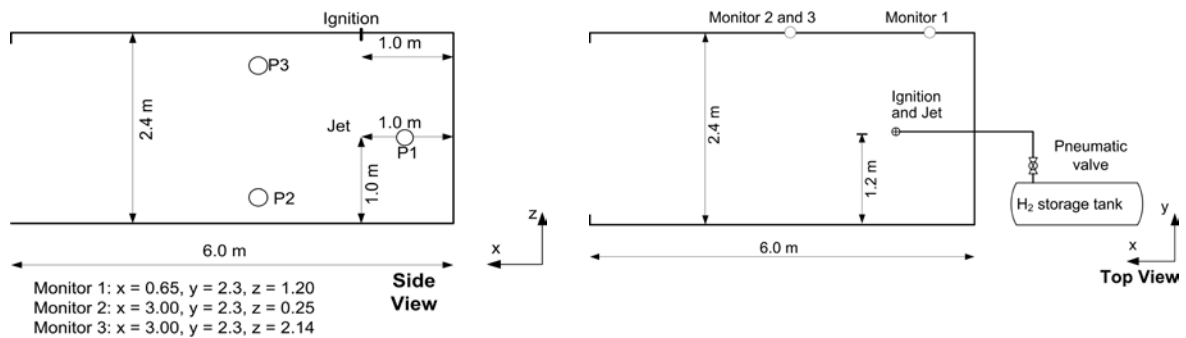


Figure 2. Side view of the container with measurements

Figure 3. Top view of the container and filling system

2.2 Fuel supply system

The fuel supply system consisted of a 0.3 m^3 storage tank and a steel tube connecting the tank and the container, shown in figure 4. The tank was placed behind the closed end wall. A nozzle was mounted at the tube outlet, experiments ranging from nozzle diameter 5, 7 and 9 mm respectively. The nozzle was placed in two different locations, 1.0 m and 3.0 m from the solid back wall at a height of 1.0 m above the container door. Different experiments were performed with the nozzle directed upwards and downwards. The storage tank was filled with hydrogen at different pressures, ranging from 0.6 to 2.4 MPa(g), and the steel container was then filled with hydrogen through the steel tube. The fuel supply was controlled by a ball valve with a pneumatic actuator. Details of the gas handling units are presented in Figure 4 and Figure 5. The fuel supply system were controlled remotely from the control room.



Figure 4. Gas storage tank and fuel supply system



Figure 5. Nozzle details, 9 mm

2.3 Instrumentation

The ignition source was a continuous spark system, built up by two electrodes and a transformer. The electrodes were mounted in the roof, 100 mm below the roof of the vessel. The ignition unit was located at two different positions during the experiments, at 1 m from the door opening, and 1 m from the closed end wall, respectively.

Three Kistler 7001 piezo-electric pressure transducers (P1, P2, P3) measured the explosion overpressure inside the container. The transducers were mounted in brass brackets sealed with silicone and were located as shown in Figure 2 and Figure 3. The pressure transducers were connected to Kistler charge amplifiers, type 5011B, from which the electrical charge was converted into a proportional voltage signal. The pressure transducers were triggered by the first input voltage signal, corresponding to the first pressure peak in the explosion. The digital logger had a built-in pre-trigger of 100 ms, allowing for a complete pressure-time development to be recorded and stored. The pressure transducers were calibrated by measuring two C-4 high explosives explosions, with 10 and 100 g of C-4 respectively. Two LC-33 pressure transducers (P4 and P5 respectively), were positioned outside the container, at several positions during the course of the experiments. P4 and P5 were mounted on steel rods, which were positioned perpendicular to the blast wave, in order to measure side-on pressure.

The hydrogen storage tank pressure was monitored with a pressure transducer mounted at the end wall of the tank. Each experiment was also recorded with two high speed video cameras. A Photron Ultima APX-RS high-speed monochrome camera with a Nikkor 50mm f/1.2 lens, was recording the explosion events at a rate of 3000 fps. The cameras were triggered manually, at the exact time as the explosion occurred, using a pre-trigger function embedded in the camera software.

2.4 Experimental matrix

From the full experiment series of 39 tests, a set of 13 successful experiments with the 9 mm nozzle are presented here, shown in Table 1. The first column in the table represent the original experiment number, the second column denotes the storage tank overpressure [MPa] prior to the release. The third column describes the nozzle direction and position from the solid end wall, and the last column show

the time of ignition [s] after the release were initiated. This matrix has a set of results where the storage tank pressure varies between 0.6 and 2.4 MPa. All but 3 of the 9 mm experiments were ignited after 15 s of hydrogen release. Table 2 presents the experimental matrix for the 4 successful experiments performed with the 5 mm nozzle. The layout is the same as for Table 1.

Table 1. Experimental matrix, 9 mm nozzle

Experiment	Initial tank pressure [MPa] (g)	Nozzle direction	Ignition [s]
23	2.0	downwards	After 15 s
24	2.0	downwards	After 15 s
25	2.0	downwards	After 10 s
26	2.4	downwards	After 15 s
27	1.2	downwards	After 15 s
28	0.6	downwards	After 15 s
29	0.6	downwards	After 16 s
30	2.0	downwards	After 15 s
35	2.0	downwards	After 7.5 s
36	2.4	downwards	After 7.5 s
37	2.4	downwards	After 15 s
38	2.4	downwards	After 15 s
39	2.4	downwards	After 15 s

Table 2. Experimental matrix, 5 mm nozzle

Experiment	Initial tank pressure [MPa] (g)	Nozzle direction	Ignition [s]
31	2.0	upwards	After 30 s
32	2.0	upwards	After 15 s
33	2.0	upwards	After 7.5 s
34	2.4	downwards	After 15 s

3.0 RESULTS AND DISCUSSION

In general most of the successful experiments were performed with a nozzle diameter of 9 mm. The time of ignition were varied from 7.5 s to 30 s, although the major part were ignited at 15 s. The direction of the nozzle were primarily downwards, but the experiment series contained both upwards and downwards directed jets. 13 successful experiments performed with the 9 mm nozzle and 4 successful experiments with the 5 mm nozzle are reported here. Not all reported experiments yielded high quality pressure recordings in all of the 5 monitor channels. As expected, the explosion overpressure increased as the initial storage tank pressure were increased.

The results are presented in topics; Nozzle size and direction, initial tank pressure, time of ignition and effect of obstructions. Apart from the section related to nozzle size, the results presented here are related to the 9 mm nozzle size only.

3.1 Nozzle configuration

4 experiments with the 5 mm nozzle were successfully performed. The time of ignition were varied from 7.5 s to 30 s. All the experiments with the 5 mm nozzle were performed in an empty container. The maximum explosion pressures were quite low, in the order of 2-4 kPa. Figure 6 shows a comparison of the 4 experiments. The figure presents the pressure records from P1, the pressure

transducer placed closest to the solid end wall. The time vectors in experiments 31, 32 and 33 have been adjusted according to experiment 34, to enable direct comparison of the data. The experiments were manually triggered, hence the experiments do not share the same zero. The results are filtered with a moving average of 10 (i.e. window size = 10), to reduce the level of noise.

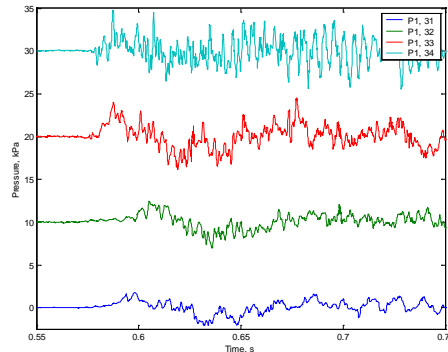


Figure 6. Pressure records from P1, experiments 31, 32, 33 and 34 (5 mm nozzle). The different experiments are separated with an offset of 10 kPa

The 5 mm nozzle experimental results are quite similar, with respect to explosion characteristics. After a short build-up the transducer record a first maximum peak. The pressure then decrease, starting a series of oscillations. The oscillating periods are in the order of 1.5 to 2.7 ms, and is quite consistent during the explosions. The other pressure transducers did not record higher maximum explosion pressures. In three of the experiments treated here, the pneumatic valve were closed as soon as the gas ignited. The remaining storage tank pressure were approximately 1000 kPa, meaning a lower level of hydrogen contributed to the explosion. This were the case for experiments 32, 33 and 34.

The results from the experiments with the 5 mm nozzle show that the explosion pressure is relatively low in this geometry. The pressure records are quite similar, even though the release times are different. In a closed container, and with ideal conditions, the mass of released hydrogen would be different due to the difference in the release times. Jet calculations imply cumulative mass of hydrogen to be 0.1 kg in the 7.5 s experiment (33), 0.19 kg for the two 15 s experiments (32 and 34) and 0.3 kg for the 30 s experiment (31). Assuming 100 % of the released hydrogen would contribute to the explosions, the explosion pressures would also be different. In the current experimental setup, this indicate that the gas cloud formed in the container have been vented out of the container during the release. As the two doors were open, the ventilation of the container was relatively good. Any release of hydrogen on the outside of the container prior to the ignition have not been detected in the high-speed films.

Experiment 30 were the only 9 mm experiment performed with the jet directed in the upwards direction. The forces acting on the steel pipe providing the gas were so strong that the pipe moved, therefore affecting the dispersion and mixing process. After the experiment were complete, the pipe were directed upwards at an angle, and the nozzle were almost close to the container roof. Due to lack of comparable data from successful experiments with the 9 mm nozzle, this paper will not discuss this topic further.

Experiments with low tank pressure (> 1.2 MPa) together with the smallest nozzle diameter (5 mm) (i.e. not reported in this paper) did not ignite at all, nor did they give visible ignition in the high speed films. In these experiments the ignition source were located 1.0 m from the container door opening.

The experimental campaign did not include 5 mm experiments with obstructions, and results from the 5 mm experiments will not be discussed further.

3.2 Initial tank pressure

The effect of initial tank pressure were investigated in experiments 26, 27, 28 and 29, where the 9 mm nozzle were directed downwards and comparable time of ignition (15 s). The initial tank pressures were 0.6 MPa in experiments 28 and 29, 1.2 MPa in experiment 27 and 2.4 MPa in experiment 26.

In test 27 a vibrating sound was detected as the explosion propagated. The test recorded a maximum pressure of 2 kPa, and the pressure slowly decreased in a time span of 1.8 s. The high-speed film from this test show flames coming out of the container. The container roof oscillated to some extent.

In test 28 the gas did not ignite, probably due to too low hydrogen gas concentration close to the ignition source. In test 29, the gas ignited after approximately 16 s, after 1 s of continuous ignition. The pressure records from the experiments with an initial tank pressure of 0.6 MPa show no clear pressure peaks, but a continuous pressure oscillation of ± 0.5 kPa. High-speed films from experiment 29 show a small blurred gas cloud and a small movement in the container floor. During the course of the experiments, it became clear that the 0.6 MPa tank pressure were the limiting case for successful ignition in this geometry.

Test 26 show a pressure rise from 0 to 2 kPa in a period of 70 ms. The first pressure peak has a maximum of 6.5 kPa, and the global maximum pressure is 14 kPa. The high-speed film from this test show flames coming out of the container, and a significant lift of the container roof.

Figure 7 shows a comparison of pressure recordings from monitor P1 between the cases where the initial tank pressure were varied from 0.6 MPa, 1.2 MPa, to 2.4 MPa (test 29, 27 and 26 respectively). It is clear that the experiment with the highest tank pressure also provide the highest explosion pressure. This can be due to the mass of hydrogen involved in the different experiments, as well as different levels of mixing. The 3 pressure monitors inside the container all gave similar results as shown in Figure 7. The far-field pressure sensors detected a pressure pulse in experiment 26 only.

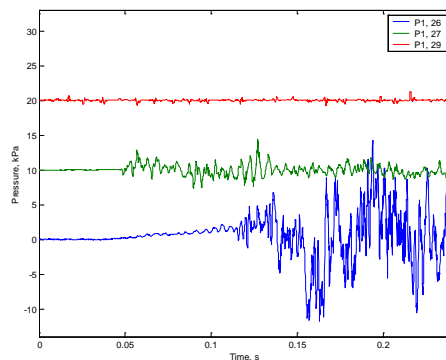


Figure 7. Pressure records of monitor P1, experiment 26, 27 and 29. The time of ignition was 15 s. The different experiments are separated with an offset of 10 kPa

Experiment 35 and 36 were ignited after 7.5 s, with an initial tank pressure of 2.0 MPa and 2.4 MPa, respectively. The high-speed films show that these explosions were fairly strong. The explosions were visible outside the container due to movement of dust on the ground. Figure 8 shows a comparison of the pressure recordings from monitor P1 from experiment 35 and 36, with an offset of 10 kPa. The pressure records show a close correlation, where the pressure build-up and overall trend in the beginning of the explosions are quite similar. In monitor P1, the maximum pressures are 8.0 kPa in both test 35 and 36. In monitors P2 and P3 the results show a similar trend. The far field pressure monitors (P4 and P5) did not record any pressure readings higher than 0.5 kPa in these two experiments.

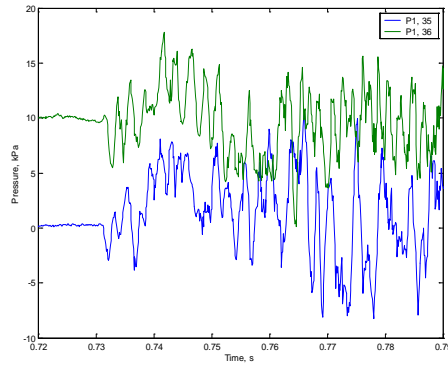


Figure 8. Pressure records of monitor P1, experiments 35 and 36. The results are separated with an offset of 10 kPa

The results show that the explosion overpressures are relatively low, despite the relatively large scale of the experiments. One probable reason for low explosion pressures could be the fact that the container was without any obstacles for the majority of the experiments. Prior to ignition, some of the hydrogen in the gas cloud could therefore be vented outside unhindered, in addition to a lower degree of turbulence and resulting pressure build-up in the explosion phase. Rai et.al. [7] have recently presented work on hydrogen gas releases in a similar shape as the ISO container, where the same effect was seen.

Time of ignition

The time of ignition was varied throughout the experimental matrix. This section presents results and discussions related to this.

Experiments 24, 25 and 35 were all done with an initial tank pressure of 2.0 MPa. The difference in the time of ignition were as follows; 7.5 s for experiment 35, 15 s for experiment 24 and 10 s for experiment 25. The maximum overpressure in experiments 24 and 25 were measured between 4 and 6 kPa, as for experiment 35 a maximum overpressure of 20 kPa was recorded. The pressure recordings in these experiments are quite similar, and show the same level of oscillations. Figure 9 shows the pressure records in monitor P1 from experiments 24, 25 and 35 (separated with an offset of 20 kPa). As expected, the results show that the later the gas cloud is ignited, the higher is the maximum explosion pressure. However, the relatively similar explosion pressures in experiments 25 and 35 may be explained by the small difference in time of ignition; after 10 s and 7.5 s, respectively. As the initial tank pressure is fairly high, there is a possibility that an amount of hydrogen gas had escaped the container prior to ignition, due to high impulse and a high degree of turbulence.

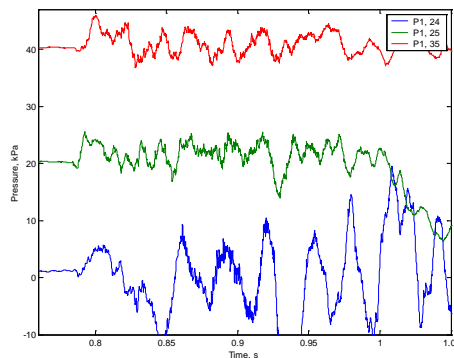


Figure 9. Pressure records of monitor P1, experiments 24, 25 and 35. The results are separated with an offset of 20 kPa

A similar comparison have been done for two experiments with an initial tank pressure of 2.4 kPa. From comparing experiments 36 and 37 the results show that the time of ignition do affect the explosion pressure. The recorded measured pressures are higher in test 37, as the time of ignition and also probably the amount of flammable gas is higher than in test 36. The comparison is visualized in Figure 10, which shows the pressure records from monitor P1. The first pressure peaks in experiments 36 and 37 have maximum at 4 kPa and 8 kPa, respectively.

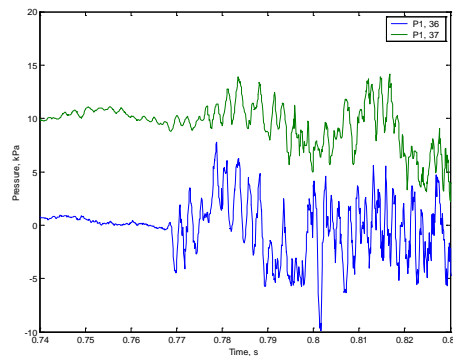


Figure 10. First pressure peaks in monitor P1, experiments 36 and 37 (offset 10 kPa)

Effect of obstructions

The effect of obstructions in the explosions have been studied by comparing the explosion pressures from experiments 26, 38 and 39. These three experiments had the same initial storage tank pressure of 2.4 MPa, but with different levels of obstructions. Test 26 had no obstructions, 28 had 2 Euro pallets and 39 had 8 Euro pallets.

Experiment 26

Experiment 26 The first pressure peak was in the order of 5 kPa inside the container, and rose to 12 kPa in the second peak. The far-field side-on pressure were 2 kPa. The high-speed film from experiment 26 show that the container roof and walls responded to the pressure build-up, and started to oscillate. The container itself moved slightly, both upwards in the open end as well as sideways in the opposite direction of the gas cloud. The pressure records from this experiment are discussed further at the end of this section, where 3 experiments are compared.

Experiment 38

In experiment 38, two wooden Euro Pallets, with dimensions 0.8 m by 1.2 m and a height of 0.12 m, were suspended from the container roof to generate turbulence during the explosion. This turbulence is mainly caused by the interaction of the flow with the obstacles. The increase in turbulence contributes to an increase in the overall burning rate, therefore creating a more violent explosion compared to an empty container. The distribution of the obstacles is shown in Figure 13.

The explosion were significantly stronger than the previous experiments. Pressure records from this test are shown in Figure 11 where the five pressure transducers are plotted with an offset of 20 kPa. The maximum pressures were 20 kPa in P1, 11 kPa in P2, and 29 kPa in P3, all measured in the first peaks. The far-field sensors P4 and P5 recorded 2.5 kPa pressure maximums. It is interesting to note that the highest pressure were recorded in P3, which were placed in the middle of the container lengthwise, and close to the roof. The innermost transducer, P1, recorded a much lower pressure. This may be due to the directionality of the explosion, as the pressure waves were directed towards the opening of the container, and away from P1, leading to a pressure build-up at P3. As the figure show, the pressure decrease after the first peak, in a series of oscillations. The pressure then increase, after 240 ms. The second pressure peak, not pictured here, were in the order of 10 kPa in P3, then

following two smaller pressure peaks successively. The high-speed film from experiment 38 show the roof lifting approximately 0.34 m as the pressure built up, based on pixel measurements. A ball of flames came out of the container during this period. After this first shock, a flame tongue exited through the container opening, and reached more than 6 m shown in Figure 12. The container were lifted to some extent. The two longest walls were bent outwards by the forces involved in the explosion, and left permanent bends along the full length of the steel wall plates.

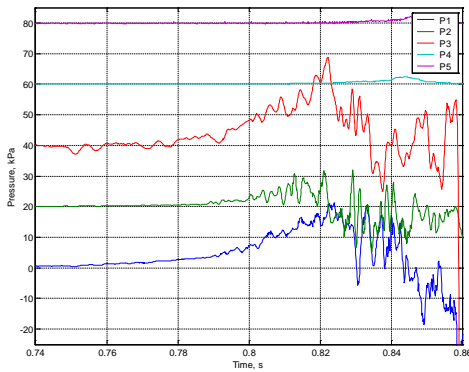


Figure 11. Pressure records from test 38, with 5 pressure transducers. The offset is 20 kPa



Figure 12. Flames in experiment 38, image from high-speed film

Experiment 39

In experiment 39, eight Euro pallets were placed inside the container to generate turbulence in the explosion. The distribution is shown in Figure 14. The nozzle was directed downwards towards one of the obstacles.

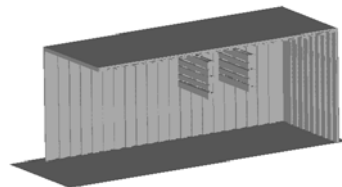


Figure 13. Distribution of obstacles in experiment 38

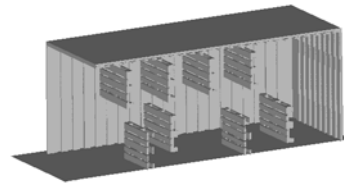


Figure 14. Distribution of obstacles in experiment 39

During this experiment, the container lifted approximately 0.5 m off ground, and therefore caused the pressure sensors located inside of the container to fail. The overpressure at the origin of the explosion is unknown. The first peak from monitor P1 was recorded though, and shows a maximum pressure of 83 kPa. The two pressure sensors located outside of the container, P4 and P5, gave pressure records as shown in Figure 15. These two sensors were located 6.5 and 8.7 meters from the container door. In the case of P4, the maximum pressure in the first peak were 16 kPa, with a rise time of 0.1 ms. The pressure then decreased to 10 kPa over a period of 1.1 ms, before the explosion generated a second pressure peak with a maximum of 24 kPa. Pressure sensor P5 recorded two peaks, similar to P4. Here the peak pressure were approximately 14 kPa at both peaks. The time of arrival of the shock wave between the first peaks in P4 and P5 were approximately 3 ms.

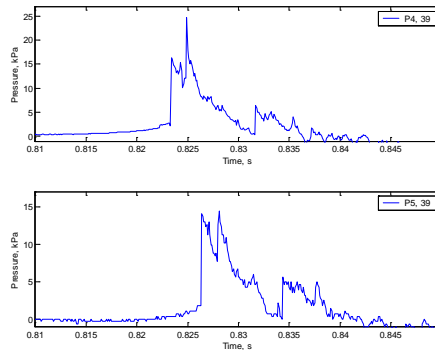


Figure 15. Pressure records from experiment 39. Pressure sensor P4 and P5 were mounted outside the container, 6.5 and 8.7 meters from the container doors

The high-speed film from experiment 39 show a violent explosion. The container walls and roof were deformed, and the stronger support beams running along the corners of the container were bent during the explosion. The curvature on the back end wall were at a maximum when the flame and explosion products become visible on the outside of the container. The welded seams along the roof and end wall were ruptured, allowing burnt gas to escape. Some of the wooden floor panels were lifted up and broken due to the explosion. Figure 16 shows the explosion in four different time steps. The trigger system involved in the pressure measurements and the trigger of the high-speed camera did not have a common zero. The first frame in the high-speed films are therefore undefined, with respect to the time of ignition and pressure build-up. The figure show the frames 460, 500, 570 and 760, corresponding to a time of 153 ms, 166 ms, 190 ms and 253 ms, respectively (counted from the first frame). Figure 16 visualize the deformation of the container, as well as the movement of the pallets used as obstructions in the explosion. Experiment 39 has been studied more thoroughly in Sommersel et.al [8] where the shock wave was treated by evaluating the high-speed films.



Figure 16. High-speed images from experiment 39, at time steps 153, 166, 190 and 253 ms, counted from camera trigger time

Figure 17 shows the pressure records from monitor P1 for experiments 26, 38 and 39. The time vectors have been adjusted to match the first peaks in each experiment. The P1 pressure transducer in experiment 39 failed later on, and the results from this experiment are therefore uncertain. The maximum pressure of 83 kPa is not shown in the figure, but nonetheless the figure show comparable initial trends in the three experiments. The P1 first peak maximum pressures were 6.5 kPa in experiment 26, 31 kPa in experiment 38 and 83 kPa in experiment 39.

The far-field pressures are presented in Figure 18 comparing results from the P5 monitor from experiments 26, 38 and 39. The pressure records show a clear pressure peak in test 39, whereas the pressure in both test 26 and 38 are comparatively low. The results from P5 show a decrease in the

measured pressure in experiment 26 after the first pressure peak; this may be noise or other kinds of error. There are therefore uncertainties related to the data from P1 in this experiment.

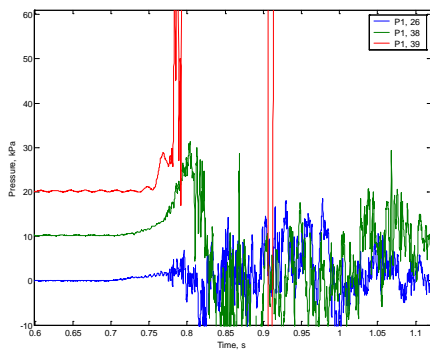


Figure 17. Comparison of pressure records from P1 in experiments 26, 38 and 39

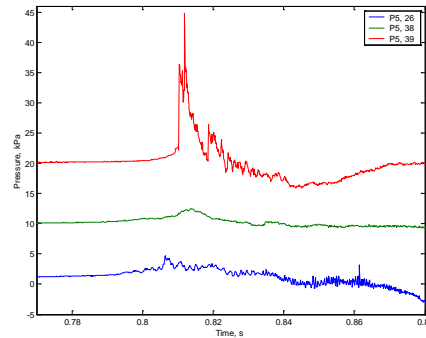


Figure 18. Comparison of pressure records from P5 (far field) in experiments 26, 38 and 39

CONCLUSIONS

Field-scale experiments were performed on pressurized releases of hydrogen inside a 6 m long ISO container, having a 2.4 m width and 2.4 m high cross section. The main objectives of these experiments were to obtain pressure and high speed data in an inhomogeneous hydrogen-air cloud. Test parameter variations included nozzle configuration, jet direction, reservoir back pressure, time of ignition after release and degree of obstacles. The results show that the experiments without obstacles were in the range of 0.4 to 7 kPa, whereas the experiments with obstacles the gas exploded more violently producing pressures in order of 100 kPa.

REFERENCES

1. Shirvill, L. C., Roberts, T.A. and Royle, M., Safety studies on high-pressure hydrogen vehicle refuelling stations: Releases into a simulated high-pressure dispensing area. *International Journal of Hydrogen Energy* **37**(8) (2012), pp.6949-6964.
2. Alcock, J.L., Shirvill, L.C., Cracknell, R.F., Compilation of existing safety data on hydrogen and comparative fuels, European Integrated Hydrogen Project II (EIHP2), deliverable report, WP 5, ENK6-CT2000-00442, (2001), Retrieved from <http://www.eihp.org/>.
3. Takeno, K., Okabayashi, K., Kouchi, A., Nonaka, T., Hashiguchi, K., Chitose, K., Dispersion and explosion field tests for 40 MPa pressurized hydrogen, *International Journal of Hydrogen Energy* **32**(13), (2007), pp.2144-2153.
4. Papanikolaou, E. A., Venetsanos, A.G. et al., HySafe SBEP-V20: Numerical studies of release experiments inside a naturally ventilated residential garage. *International Journal of Hydrogen Energy* **35**(10), 2010, pp.4747-4757.
5. Giannissi, S.G., Shentsov, V., Melideo, D., Cariteau, B., Baraldi, D., CFD benchmark on hydrogen release and dispersion in confined, naturally ventilated space with one vent, *International Journal of Hydrogen Energy*, **40**(8), 2015, pp. 2415-2429.
6. Middha, P. and Hansen, O.R., Using computational fluid dynamics as a tool for hydrogen safety studies, *Journal of Loss Prevention in the Process Industries*, **22**(3), 2009, pp.295-302.

7. Rai, K., Bjerketvedt, D. and Gaathaug, A.V., Gas explosion field tests with release of hydrogen from a high pressure reservoir into a channel, *International Journal of Hydrogen Energy*, 39(8), 2014, pp. 3956-3962.
8. Sommersel, O., Bjerketvedt, D., Christensen, S., Krest, O. and Vaagsaether, K., Application of background oriented schlieren for quantitative measurements of shock waves from explosions, *ShockWaves*, 18(4), 2008, pp.291–297.